AD-A182 020 IR LIQUID SWITCH VOLUME 1(U) MARTIN MARIETTA LABS BALTIMORE MD W CHEN ET AL OCT 86 MML-TR-86-85C-VOL-1 DAAK70-84-C-0022 1/1

UNCLASSIFIED F/G 20/6 NL

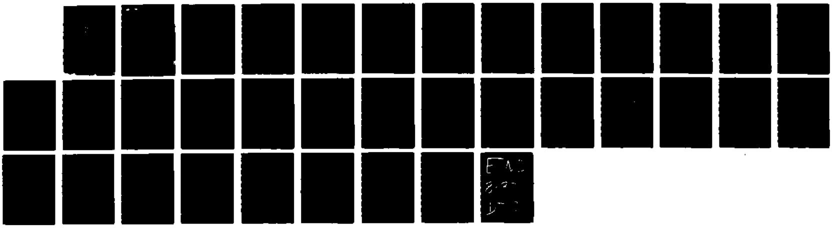

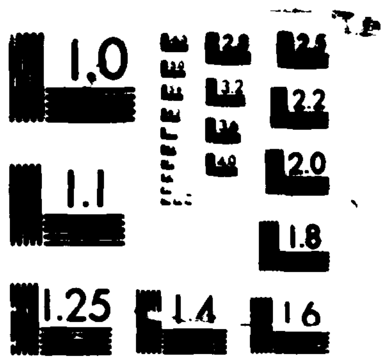

MICROCOPY RESOLUTION TEST CHART

MARTIN MARIETTA

UNCLASSIFIED

SECURITY CLASSIFICATION OF THIS PAGE (When Data Entered)

REPORT DOCUMENTATION PAGE		READ INSTRUCTIONS BEFORE COMPLETING FORM
1. REPORT NUMBER	2. GOVT ACCESSION NO. AD-A182020	3. RECIPIENT'S CATALOG NUMBER
4. TITLE (and Subtitle) "IR LIQUID SWITCH" FINAL REPORT (VOLUME I)		5. TYPE OF REPORT & PERIOD COVERED FINAL REPORT 4/18/84 - 7/31/86
		6. PERFORMING ORG. REPORT NUMBER MML TR 86-85(c)
7. AUTHOR(s) Wenpeng Chen, Claude Frazier, and Jar-Mo Chen		8. CONTRACT OR GRANT NUMBER(s) DAAK70-84-C-0022
9. PERFORMING ORGANIZATION NAME AND ADDRESS Martin Marietta Corporation, Martin Marietta Laboratories, 1450 S. Rolling Road, Baltimore, MD 21227-3898		10. PROGRAM ELEMENT, PROJECT, TASK AREA & WORK UNIT NUMBERS
11. CONTROLLING OFFICE NAME AND ADDRESS U.S. Army Electronics R&D Command, Night Vision and Electro-Optics Laboratory, Ft. Belvoir, VA 22060		12. REPORT DATE October, 1986
		13. NUMBER OF PAGES 31
14. MONITORING AGENCY NAME & ADDRESS (if different from Controlling Office)		15. SECURITY CLASS. (of this report) UNCLASSIFIED
		15a. DECLASSIFICATION DOWNGRADING SCHEDULE

16. DISTRIBUTION STATEMENT (of this Report)

Distribution unlimited - Approved for Public Release

17. DISTRIBUTION STATEMENT (of the abstract entered in Block 20, if different from Report)

18. SUPPLEMENTARY NOTES

19. KEY WORDS (Continue on reverse side if necessary and identify by block number)

nonlinear optical materials, photothermal effect, artificial Kerr effect, self-defocusing, and nonlinear interface.

20. ABSTRACT (Continue on reverse side if necessary and identify by block number)

In recent years, nonlinear optical materials having large nonlinear optical coefficients when combined with novel optical mechanisms have found many applications in the field of phase conjugation, image processing, optical computing, and optical switching. We have analyzed two dynamic nonlinear optical effects, artificial Kerr and photothermal, and reviewed two nonlinear phenomena, self-defocusing and nonlinear interface. The generic results are discussed ~~here~~. Please see Volume II for their device applications. (See reverse.)

DD FORM 1 JAN 73 1473 EDITION OF 1 NOV 65 IS OBSOLETE

UNCLASSIFIED

SECURITY CLASSIFICATION OF THIS PAGE (When Data Entered)

20. Abstract

We concluded that both AKM and absorptive liquid mixtures are highly nonlinear optical materials. The photothermal effect of the latter is about three orders of magnitude higher under the same focus condition. And both the self-defocusing and nonlinear-interface phenomena produce a response faster than 100 μs under reasonable power levels. In addition, the dynamic nonlinear coefficient n_2' of AKM is derived. We found that (1) the figure of merit of AKM should be defined as $n_2/\alpha_o\lambda_o$ and not the n_2/α_o originally used in literature because α_o cannot be infinitely increased; and (2) the dynamic nonlinear coefficient n_2' is larger for smaller spheres under the constraint of the same scattering loss.

MML TR 86-85c

QUALITY INSPECTED 1

IR LIQUID SWITCH

Final Report (Volume I)

Accession For	
NTIS GRA&I	☒
DTIC TAB	☐
Unannounced	☐
Justification	
By	
Distribution/	
Availability Codes	
Dist	Avail and/or Special
A-1	

October 1986

Prepared for

U.S. Army Electronics R&D Command
Night Vision and Electro-Optics Laboratory
Attn: DELNV-R (Wood)
Fort Belvoir, VA 20060

Prepared by

Wenpeng Chen, Claude Frazier, and Jar-Mo Chen
MARTIN MARIETTA CORPORATION
Martin Marietta Laboratories
1450 South Rolling Rd.
Baltimore, MD 21227-3898

TABLE OF CONTENTS

LIST OF FIGURES

FOREWORD

This document is the first volume of the Final Report (two volumes) of Contract No. DAAK70-84-C-0022, "IR Artificial Kerr Media," from U.S. Electronics R&D Command, Night Vision and Electro-Optics Laboratory (NV&EOL). The work was performed by W.P. Chen and C.C. Frazier with the assistance of H. Jones, M.A. Harvey, L.M. Gillette, M.P. Cockerham, and P.L. Porter during the period 18 April 1984 to 31 July 1986 under the management of J.M. Chen.

The authors are grateful to G. Wood, E. Sharp, and R. Shurtz* of NV&EOL for their support, encouragement, and fruitful discussion. They also wish to acknowledge M. Kroll for pointing out the thermal lensing phenomenon and S. Guha for elucidating it.

* Now with BDM

I. INTRODUCTION

In recent years, nonlinear optical materials having large nonlinear optical coefficients when combined with novel optical mechanisms have found many applications in the field of phase conjugation, image processing, optical computing, and optical switching.[1] In this volume of the Final Report we will discuss two types of nonlinear materials, artificial Kerr medium (AKM) and liquid mixture; and two types of nonlinear optical mechanisms, self-defocusing and nonlinear interface.

II. NONLINEAR MATERIALS

A. ARTIFICIAL KERR MEDIUM

An artificial Kerr medium is a suspension of transparent particles in a transparent liquid of a different refractive index.[2] A focused laser beam can exert substantial radiation pressure on the particles and cause nonlinear effects. Under the influence of such pressure, the particles redistribute (Fig. 1).

When a dielectric particle is in an electrical field $\vec{E}$, it behaves like a dipole with a polarization $\vec{P}$ given by[3]

$$\vec{P} = p\vec{E} \qquad (1)$$

where p is the effective polarizability of the particle. For a sphere, the p is given by

$$p = n_{\ell}^{2} \left(\frac{n_r^{2} - 1}{n_r^{2} + 2}\right) a^{3} \qquad (2)$$

where $n_r = n_s/n_{\ell}$ is the ratio of the refractive indices of the sphere (n_s) and the liquid (n_{ℓ}) and a is the radius of the sphere. The sphere experiences a force due to the optical field gradient given by[4]

$$\vec{F} = (\vec{P} \cdot \nabla)\, \vec{E} = (1/2)\ p\ \nabla\vec{E}_o^{\,2} \equiv -\nabla\phi \qquad (3)$$

and

$$\phi = -\frac{1}{2}\, p\ \vec{E}_o \cdot \vec{E}_o \qquad (4)$$

where E_o is the time-averaged rms electric field of the light wave and ϕ is the light-induced potential.

For a light beam incident onto a liquid suspension of spheres, the optically induced force moves the spheres with $n_s > n_{\ell}$ and $n_s < n_{\ell}$ into and out of the high-optical-intensity region, respectively. In both cases, the

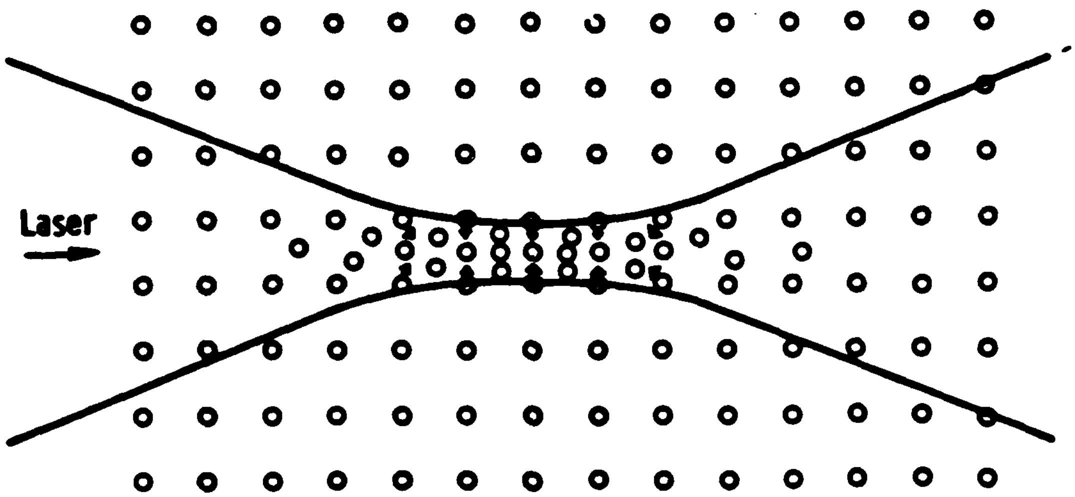

Figure 1. Schematic diagram of an artificial Kerr medium. Particles at the focus are moved by the optical dipole force to change the refractive index.

motion of the spheres creates refractive index changes which are analogous to those in a medium with a positive optical Kerr coefficient, and the effective refractive index for the suspension system is given to a good approximation, as long as $f \ll 1$, by

$$n_{medium} = n_\ell + f\,(n_s - n_\ell) \qquad (5)$$

where $f\ (= \frac{4\pi}{3} a^3 N)$ is the volume fraction of the spheres, and N is the number of spheres per unit volume. For $f < 0.1$, the n_{medium} given by Eq. (5) will deviate from that derived from the more accurate Maxwell-Garnet theory by no more than 2%.

For application of this medium as an optical switch, the scattering loss associated with the nonlinear effect must also be considered. When the radius of the spheres is much less than the wavelength of the incident light, the scattering loss per unit length, α_o, is given by the Rayleigh formula(5)

$$\alpha_o = \frac{32\pi^4\, n_\ell^4}{\lambda_o^4} \left(\frac{n_r^2 - 1}{n_r^2 + 2}\right)^2 a^3 f \qquad (6)$$

where λ_o is the wavelength of the incident light in vacuum. One figure of merit of the medium is the ratio of its nonlinear coefficient to its scattering loss. This will be discussed in the following sections for the static and dynamic cases. We can rewrite Eq. 6 as

$$\alpha_o\ \lambda_o = 32\pi^4 n_\ell^4 \left(\frac{n_r^2 - 1}{n_r^2 + 2}\right)^2 \left(\frac{a}{\lambda_o}\right)^3 f \qquad (7)$$

As we keep f constant and scale a with λ_o, the $\alpha_o\lambda_o$ can be kept constant.

1. Continuous-Wave (Static) Case

In the static case, the flow of the spheres induced by the optical field is counterbalanced by thermal diffusion. At equilibrium, the ratio of N inside and outside the beam is proportional to $\exp(-\phi/kT)$, where ϕ is the optically induced potential inside the beam relative to that outside

and is proportional to the optical power density I of the light beam. Usually, $\phi \ll kT$, and we can expand $\exp(-\phi/kT)$ as $(1-\phi/kT)$. Thus, the optically induced difference in the sphere density is $\sim N\phi/kT$, and

$$n_{medium} = n_\ell + \frac{4\pi}{3} a^3 N (n_s - n_\ell) - \frac{4\pi}{3} a^3 (n_s - n_\ell) \frac{N\phi}{kT} . \quad (8)$$

Because $\phi \propto I$, the third term in the equation describes the effective optical Kerr effect. The static effective optical Kerr coefficient n_2 is then given by[6]

$$n_2 = 2\pi \frac{n_\ell^2}{ckT} \frac{(n_r^2 - 1) a^3 f}{(n_r + 1)(n_r^2 + 2)} . \quad (9)$$

When the n_2 is normalized to the α_o (scattering loss) and the $\alpha_o \lambda_o$ to derive the figure of merit, we obtain:

$$\frac{n_2}{\alpha_o} = \frac{\lambda_o^4}{16\pi^3 ckTn_\ell^2} \left(\frac{n_r^2 + 2}{n_r + 1}\right) \quad (10a)$$

$$\frac{n_2}{\alpha_o \lambda_o} = \frac{\lambda_o^3}{16\pi^3 ckTn_\ell^2} \left(\frac{n_r^2 + 2}{n_r + 1}\right) . \quad (10b)$$

Note that the proportionalities n_2/α_o and $n_2/\alpha_o\lambda_o$ vary as <u>the fourth and third power of the wavelength, respectively</u>. As long as the scattering loss is kept constant, n_2 is independent of a, and the redistribution of spheres is determined by the thermal equilibrium. Therefore, the resultant static n_2 depends on temperature and the optically induced potential difference, and not on the field pattern of a focused light beam.

2. Pulse Case

The field pattern does play an important role in the pulse case, because the steepness of the field gradient determines the forces on the spheres and their accelerations. When a TEM_{00} laser beam is focused as shown in Fig. 2, the field pattern at any plane z, expressed in Gaussian units, is

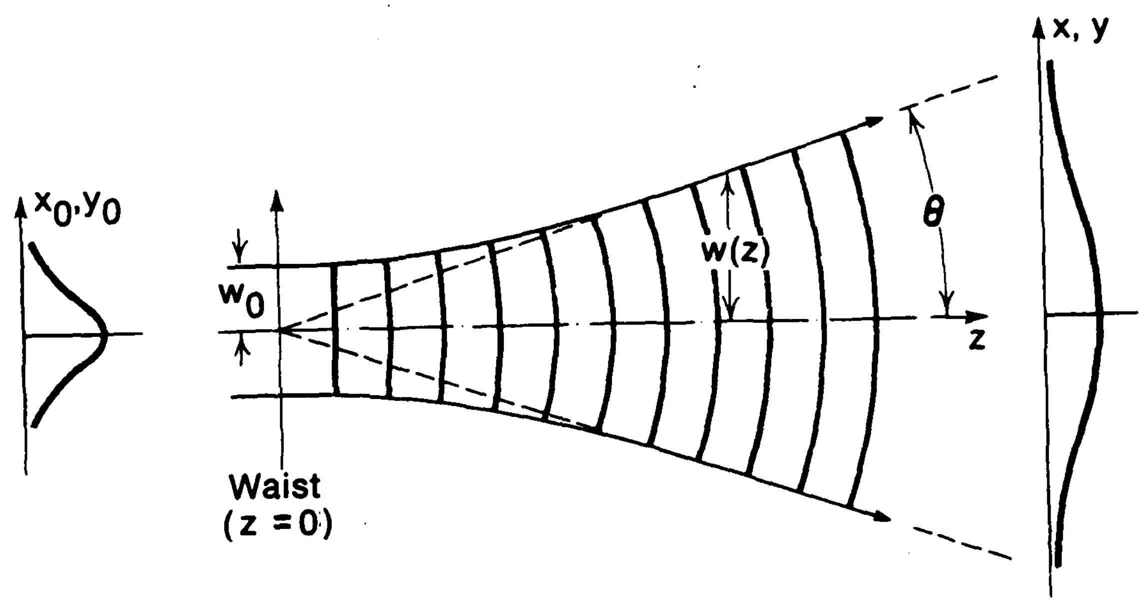

Figure 2. Schematic diagram showing the optics for calculating the dynamic nonlinear coefficient of an AKM. (From Ref. 7.)

$$\vec{E} = \left(\frac{8\pi}{cn} P'\right)^{1/2} \tilde{\mu}\hat{x} \tag{11}$$

$$\tilde{\mu}(r,z) = \sqrt{\frac{2}{\pi}}\ \frac{1}{w(z)} \exp\left\{-j\ [kz - \psi(z)]\right\} \exp\left[-j\ \frac{k}{2}\ \frac{r^2}{\tilde{q}(z)}\right]. \tag{12}$$

At the focal spot (z=0), $\mu(r,o)$ is

$$\tilde{\mu}_o(r) = \sqrt{\frac{2}{\pi}}\frac{1}{w_o} \exp\left(-j\ \frac{k}{2}\ \frac{r^2}{\tilde{q}_o}\right) \tag{13}$$

where P' = total input power

n = refractive index of the medium at low-power irradiation

c = speed of light

w_o = radius of the beam at the focal spot

$k = 2\pi/\lambda$

$\lambda = \lambda_o/n$

$\tilde{q}(z) = \tilde{q}_o + z$

$\tilde{q}_o = j\ \pi w_o^2/\lambda \equiv jz_R$

z_R = the Rayleigh length; at $z = \pm z_R$, $w = \sqrt{2}\, w_o$

$$\frac{1}{\tilde{q}(z)} = \frac{1}{R(z)} - \frac{\lambda}{\pi w^2(z)}$$

$$R(z) = z + \frac{z_R^2}{z} = z\ \left[1 + \left(\frac{z_R}{z}\right)^2\right]$$

$$w(z) = \omega_o \sqrt{1 + \left(\frac{z}{z_R}\right)^2}$$

$$\psi(z) = \tan^{-1}\left(\frac{z}{z_R}\right)$$

$$\iint |\tilde{\mu}_o|^2\ 2\pi r dr = 1.$$

The field pattern in the region $z < 0$ is a mirror image of that for $z > 0$ at the plane z=0. When a laser beam with beam diameter D is focused by a lens with focal length L, the w_o is given by

$$w_o = \frac{2\lambda_L}{\pi D} \tag{14}$$

provided $\frac{2\lambda_L}{\pi D} << 1$.

Now, from Eq. (3), we can calculate force as

$$\vec{F} = \frac{1}{2}\, p\, \nabla E_o^{\,2} = \frac{-2pr\ |E_o|^2}{w_o^{\,2}\left[1 + (\frac{z}{z_R})^2\right]^2}\ \hat{r} - \frac{p\,\frac{z}{z_R^{\,2}}}{1 + (\frac{z}{z_R})^2} \cdot \left\{1 - \frac{2r^2}{w_o^{\,2}\left[1 + (\frac{z}{z_R})^2\right]}\right\} |E_o|^2\ \hat{z}. \tag{15}$$

Along the optical axis (r=0), the force is only in the z direction and towards the focal point, with maxima occurring at $|z| = \frac{1}{\sqrt{3}} z_R$. At the focal plane (z=0), the force is only on the plane and towards the focal point, and a maximum occurs at $r = 0.5\ w_o$. In a situation where a sample is thinner than z_R and locates at z=0, the force is mainly in the radial direction.

Substituting p from Eq. (2) into the first term of Eq. (15), we can explicitly derive the force at z=0 as

$$|F| = \left[\frac{32}{cn}\, n_\ell^{\,2} \left(\frac{n_r^{\,2} - 1}{n_r^{\,2} + 2}\right)\right] a^3 \left.\right] \frac{r}{w_o^{\,4}} \exp\left(-\frac{2r^2}{w_o^{\,2}}\right) P' \equiv \tag{16}$$

$$\equiv A a^3\, \frac{r}{w_o^{\,4}} \exp\left(-\frac{2r^2}{w_o^{\,2}}\right) P'$$

with the force toward the center and A equal to the value in the bracket. In cgs units, the equation of motion of the spheres is given by

$$m\ddot{r} = -6\ \pi a\ \eta\dot{r} - A\ a^3\, \frac{r}{w_o^{\,4}} \exp\left(-\frac{2r^2}{w_o^{\,2}}\right) P' \tag{17}$$

where m is the mass of the spheres and η is the coefficient of viscosity. The first term on the righthand side of Eq. (17) is the viscosity force.

In the region $r < 0.5\ w_o$, where the force is significant, Eq. (17) can be approximated as*

$$\ddot{r} = -\frac{6\pi a\eta}{m}\ \dot{r} - \frac{Aa^3}{m}\ \frac{r}{w_o^4}\ P' \equiv$$

$$\equiv \delta\dot{r} + \beta r. \tag{18}$$

The force due to light is overestimated by Eq. (18), so that the actual response will be slower than the calculated one. In the cases that we are likely to encounter, namely, $a < 2\ \mu m$ and $w_o > 3\ \mu m$, then $4\ \beta << \delta^2$, and the solution to Eq. (18) becomes simply

$$r = r_i e^{-(\beta/\delta)t} = r_i\ (1 - \frac{\beta}{\delta}\ t) \tag{19}$$

where r_i is the initial position of the sphere at the onset of the pulse.

Now, we can estimate the change of density of the spheres in the region $r < 0.5\ w_o$ as a function of time as follows. All of the spheres originally located within a distance r_i from the origin move to within a distance r_f, given by

$$r_f = r_i\ (1 - \frac{\beta}{\delta}\ t). \tag{20}$$

Therefore, the density within r_f increases by

$$\Delta N = \frac{(\pi r_i^{\ 2} - \pi r_f^{\ 2})\ N}{\pi r_f^{\ 2}} = N\ (2\ \frac{\beta}{\delta}\ t). \tag{21}$$

The resulting change in the refractive index is

---

* First pointed out by G. Wood at NVEOL.

$$\Delta n = \Delta N \, (n_s - n_\ell) \frac{4}{3} \pi a^3 =$$

$$= \frac{8\pi}{3} a^3 (n_s - n_\ell) \frac{\beta}{\delta} Nt. \tag{22}$$

Substituting δ and β from Eq. (18) and N from Eq. (6) with $f = \frac{4\pi}{3} a^3 N$ into Eq. (22), we have

$$\Delta n = \frac{1}{6\pi^4 n_\ell^2} \left(\frac{n_r^2 + 2}{n_r + 1} \right) \frac{1}{c\eta} \frac{\lambda_o^4}{a w_o^2} \, t \, I\alpha_o \text{ (in cgs units)} \tag{23}$$

where

$$I \equiv \frac{2}{\pi w_o^2} P'$$

is the average power density. Using the relationship $\Delta n = n_2' I$ and rearranging the equation, we obtain

$$\frac{n_2'}{\alpha_o \lambda_o} = \frac{1}{6\pi a \eta} \frac{16}{w_o^2} \left[\frac{1}{16\pi^3 c} \frac{\lambda_o^3}{n_\ell^2} \left(\frac{n_r^2 + 2}{n_r + 1} \right) \right] t \tag{24}$$

where n'_2 is the dynamic nonlinear coefficient.

Like the figure of merit of the CW nonlinear effect, $n_2/\alpha_o\lambda_o$ (Eq. 10), $n'_2/\alpha_o\lambda_o$ is a function of λ_o, n_ℓ, and n_r. However, it depends on the viscosity and the beam width instead of the temperature. It should be noted that the response becomes faster as the sphere becomes smaller.

We can illustrate this effect by calculating the responses for AKM with the following parameters: $n_\ell = 1.5$, $n_s = 2.35$, $\eta = 0.02$ g sec^{-1}cm^{-1}, and $\alpha_o = 15$ cm^{-1}. A 100-μm-thick layer of this medium would cause only a 14% scattering loss. With the parameters given, the product $a^3 f$ is then fixed by Eq. (6) for a given wavelength λ_o. A small radius will be selected to produce fast response. However, since the volume fraction f cannot exceed 100%, there exists a lower bound of the radius a which, for this case, is ~ 2200 Å. So, if we take a = 2200 Å, then the Δn vs/t curve given by Eq. (24) and shown in Fig. 3 sets the optimum response of the AKM for a 0.38-W CO_2 laser focused to a 40-μm diameter.

B. LIQUID MIXTURE

A liquid mixture can have a very large dynamic nonlinear effect. However, the effect was not appreciated in connection with optical switching limitation applications. Absorption of incident light upon a liquid can heat up the liquid and change its refractive index. In regions of the optical spectrum far removed from the absorption bands of the liquid and at temperatures away from phase changes or critical points of the liquid, the temperature coefficient of the index of refraction, $dn/dT(K^{-1})$,

$$dn/dT = (\partial n/\partial T)_{\rho} + (\partial n/\partial \rho)\,(\partial \rho/\partial T) \tag{25}$$

is determined primarily by changes in the sample density (second term). Most liquids expand when heated, resulting in a negative value of dn/dT.

The thermally-induced change in n can be estimated from the heat produced by the absorption. The power, P_{trans}, (W) transmitted through a thickness, ℓ, (cm) of a sample with absorptivity, α, (cm^{-1}) is given as

$$P_{trans} = Pe^{-\alpha\ell} \tag{26}$$

where P (W) is the incident power. For $\alpha\ell \ll 1$, the absorbed power is approximately

$$P_{abs} = P - P_{trans} = P\alpha\ell \ . \tag{27}$$

Consider the situation of a laser focusing to a waist w upon a sample with $\alpha = 15\ cm^{-1}$ and $\ell = 100\ \mu m$. The absorption is ~14%. The rate of energy delivery to the sample, Q_{in}, is $P\alpha\ell/J$, where $J = 4.18\ J\ cal^{-1}$ is Joule's constant. We assume complete dissipation of the incident energy as heat. The rate of temperature increase, $\dot{T}$, is

$$\dot{T} = P\alpha\ell/J\pi w^2\ \ell\rho C_p = \left(\frac{\alpha}{J\rho C_p}\right)\left(\frac{P}{\pi w^2}\right) \equiv \frac{\alpha}{J\rho C_p} I \tag{28}$$

depending on the sample volume $\pi w^2 \ell (cm^3)$, the specific heat C_p (cal g^{-1} K^{-1}), and the sample density $\rho (g\ cm^{-3})$. The heat is then conducted radially from the illuminated region into its surroundings. The thermal conductivity κ (cal sec^{-1} cm^{-1} K^{-1}) relates Q_{out}, the time rate of heat transfer by conduction to the surface area, in the present case $2\pi w \ell$, to the distance ($\sim w$) between the heated spot and its surroundings, and to the difference in temperature ΔT; hence $Q_{out} = (\kappa)\ (2\pi w \ell)\ (\Delta T)/w$.

When the sample temperature reaches an equilibrium value, $Q_{in} = Q_{out}$. At the rate of temperature increase $\dot{T}$ calculated above, equilibrium would be achieved in a time

$$\Delta t = \Delta T/\dot{T} = [(P\alpha\ell/J)w/\kappa_2 \pi w \ell]/(P\alpha\ell/J\pi w^2 \ell \rho C_p) = {}^1\!/_2\, w^2 \rho C_p/\kappa.$$

The expression for Δt above represents a fundamental time for determining whether the heat conduction shall or shall not be taken into consideration. For a pulse shorter than Δt, we can ignore the conduction loss. Of course, these calculations cannot be taken too literally and are only meant to provide an appreciation for the order of magnitude of the effects being considered here. Detailed analysis can be found in Ref 8.

Using liquid benzene with some dye as a typical organic sample, where $\ell = 0.88\ g\ cm^{-3}$, $C_p = 0.41$ cal $g^{-1}K^{-1}$, and $\kappa = 3.41 \times 10^{-4}$ cal $sec^{-1}cm^{-1}K^{-1}$,[9] and assuming that dn/dT in the IR region is the same as that in the visible, $dn/dT = -3.9 \times 10^{-4}\ K^{-1}$,[10] we can estimate the $\dot{T}$ and Δt for a 1-W laser focused to an area of 1 cm^2. The resultant $\dot{T}$ is ~ 9.95 K sec^{-1}. For the case of short laser pulses in which we can ignore conduction, the $\dot{T}$ will cause a decrease of n given by

$$\dot{n} = -3.9 \times 10^{-3}\ (W/cm^2)^{-1} sec^{-1}. \tag{29}$$

The change in refractive index, Δn, of the sample is isotropic. The Δn vs t curve (curve a) of the typical example is also shown in Fig. 3 and can be compared with the corresponding AKM curve. We see that the photothermal effect is at least three orders of magnitude higher than the artificial

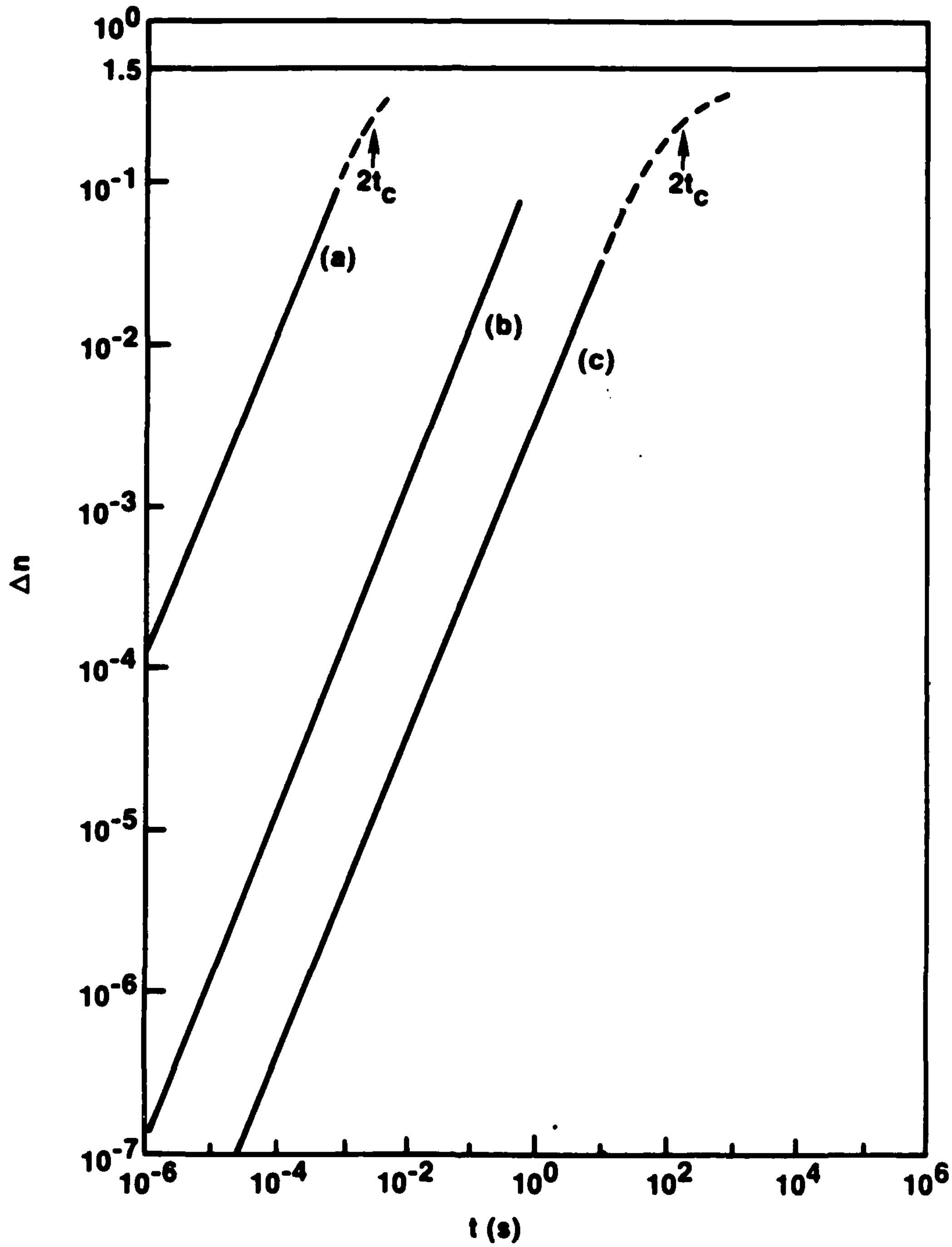

Figure 3. The estimated Δn vs t curves for a 0.38-W CO_2 laser focused at 40-μm diameter a) in a liquid mixture and b) in an AKM. c) A corresponding curve for a 1 W/cm^2 power density in the liquid mixture. Specifications of the liquid mixture and the AKM are given in the text.

Kerr effect at the same response speed. Also shown is the Δn vs t curve (curve c) at $1 W/cm^2$ power level. It is worth noting that the photothermal effect (for $t > 1$ msec) is comparable to the strong nonlinear optical effect in a semiconductor at the band edges. For example, n_2 of $Hg_{0.8}Cd_{0.2}Te$ (having $\lambda_g = 7.5$ µm and $\alpha = 26$ cm^{-1} at 10.6 µm) is 8×10^{-8} $(W/cm^2)^{-1}$ for 180 nsec pulses and is estimated to be $\sim 1.2 \times 10^{-6}$ $(W/cm^2)^{-1}$ at steady state.[11] In fact, the photothermal effect can be 10 times larger if a sample has 10 times larger α. For laser lines that fall into the absorption band of a mixture, the dn/dT may be enhanced due to a resonant effect.

III. NONLINEAR OPTICAL MECHANISMS

Nonlinear self-focusing/defocusing and nonlinear interface will be discussed in this section. Because the nonlinear effect of an AKM is about three orders of magnitude slower than the photothermal effect at the same response speed, we will only use the latter as an example. The results can be qualitatively applied to the cases involving AKM, as long as the time scale is increased according to their difference in response.

A. SELF-DEFOCUSING[8]

When a thin sample of liquid mixture is exposed to a pulsed laser producing a TEM_{00} laser beam with a radially symmetric Gaussian intensity distribution (Fig. 4), the sample is most strongly heated at the center of the beam, where the intensity is greatest, and consequently forms a lens-like optical element. For most materials, the increase in temperature lowers the refractive index so that the optical path is shorter at the beam center, i.e., it is equivalent to a divergent lens.

As shown in the literature, the thermally induced effect is time dependent; the lens requires a finite time to reach a steady-state condition. The steady-state focal length, $f(\infty)$, of a thermal lens produced by a Gaussian laser beam of spot size, w_1^2 , at the sample has been derived:[12,13]

$$f(\infty) = \frac{\pi J \ \kappa w_1^2}{P(dn/dT)\alpha \ell} \tag{30}$$

where J, k, P, (dn/dT), α, and ℓ are defined as before. This expression assumes that all of the abosrbed radiation is converted to heat. As the thermal lens approaches steady state, its focal length f(t) is characterized [12] by the following expression:

$$f(t) = f(\infty)\ (1 + t_c/2t) \tag{31}$$

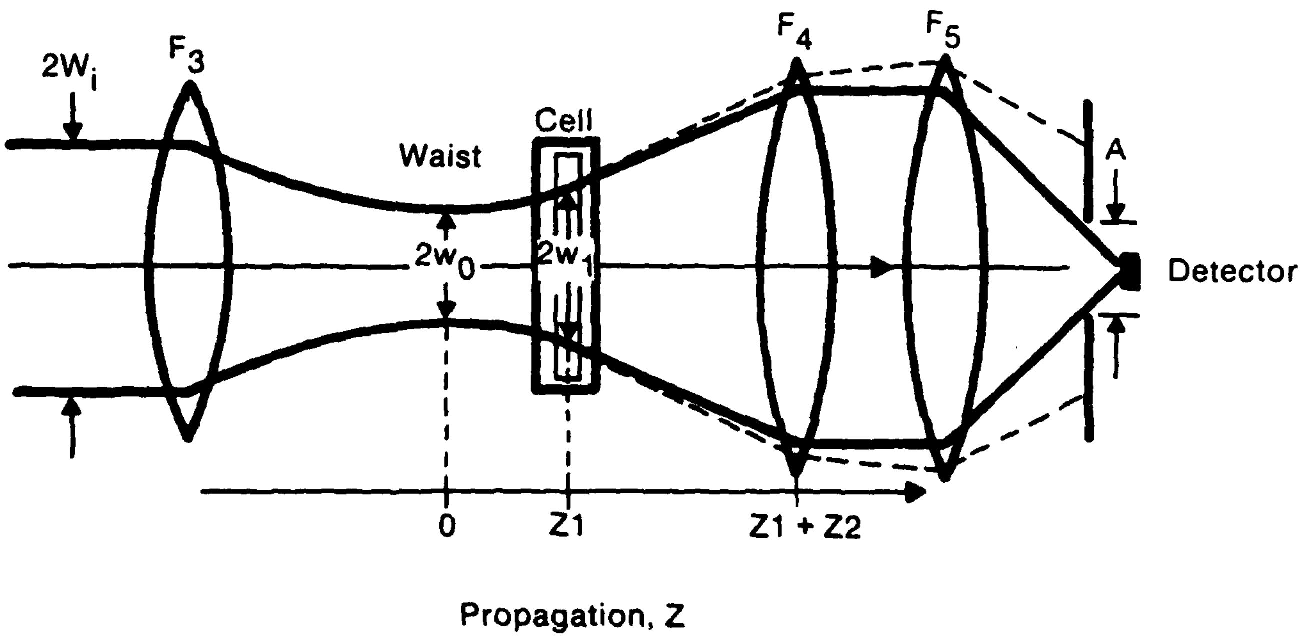

Figure 4. Optical configuration for calculating the focal length of a thermal lens and the transmission through aperture A.

where t_c is a time constant given by:

$$t_c = \frac{w_1^2 \rho C_p}{4\kappa} \tag{32}$$

and ρ and C_p are defined as before. Characteristic time constants are in the range of tens of microseconds to several seconds,[14] depending on the spot size of the laser beam and the thermal properties of the sample.

Although the magnitude of t_c at first appears hopelessly long for an ns switching application, the time needed to reduce transmission to a safe level can be much faster. Using the optical configuration shown in Fig. 4, we were able to calculate the time-dependent reduction of transmission through an aperture A for a 1-W laser focusing to a spot 20 µm in radius on a 100-µm sample. The sample was assumed to have properties similar to benzene, except for the absorption coefficient. Also, heat transfer from the liquid to the sample cell was not considered. The transmission for A = 0.002 and 0.055 cm was estimated to drop to < 50% in less than 1 and 24 µs, respectively (Fig. 5).

For the case under consideration, i.e., $t \ll t_c$, f(t) becomes

$$f(t) \simeq f(\infty)\, t_c/2t = \frac{\pi J\, w_1^4\, \rho c_p}{8P(dn/dT)\alpha\ell}\,\frac{1}{t} \tag{33}$$

i.e., the response is proportional to w_1^4, ρ, and c_p, and inversely proportional to P, dn/dT, α, and ℓ. Very short switching times are possible by properly combining these parameters.

B. NONLINEAR INTERFACE[15]

While the self-defocusing mechanism requires a focused beam to provide lens-like effect, the nonlinear-interface effect can deal with broad beams. Consider an infinite plane wave incident upon a plane boundary separating two different optical media: a linear medium a and a nonlinear medium b (Fig. 6). In addition to the incident wave, there will

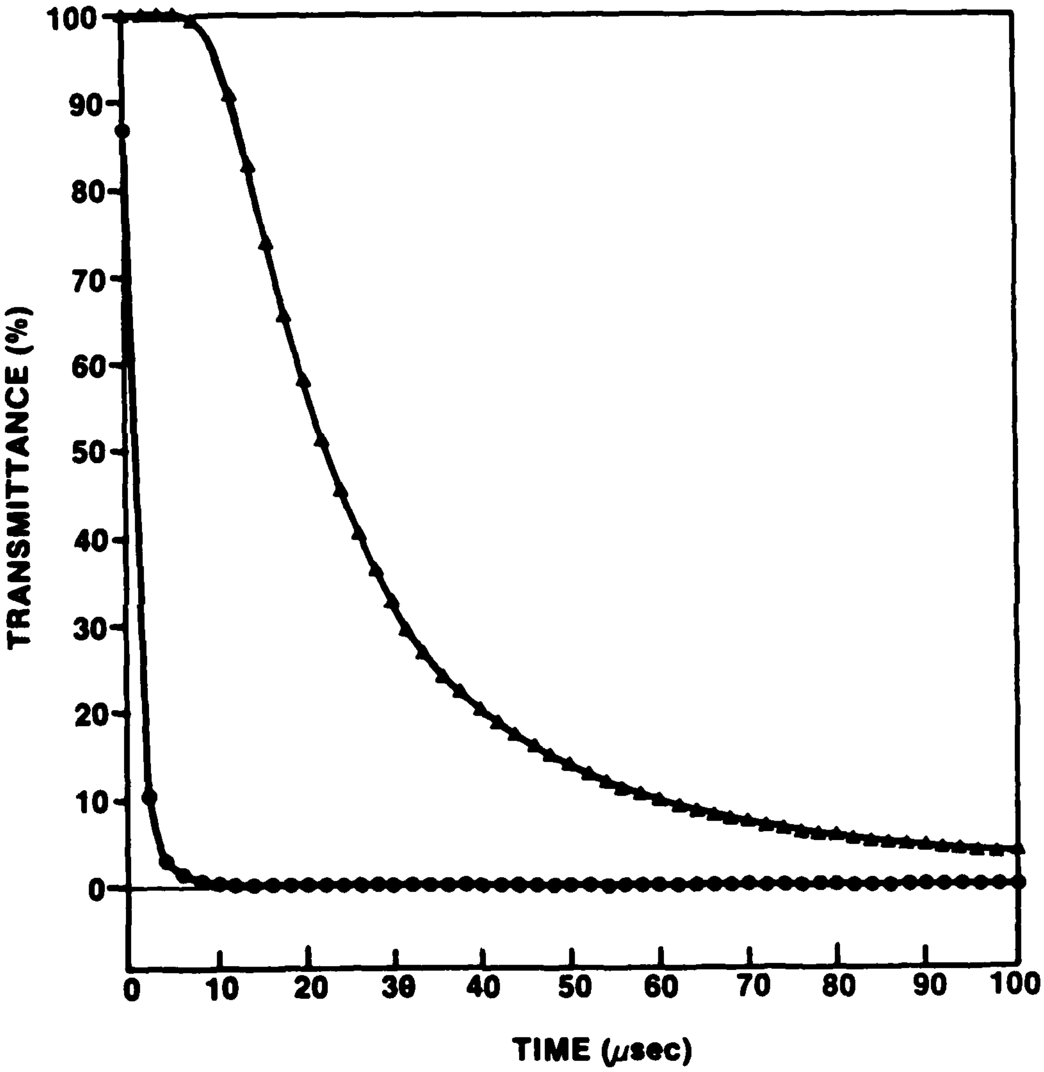

Figure 5. Dynamic nonlinear transmission through aperture A in Fig. 4 due to thermally induced self-defocusing for A = 0.055 (upper curve) and 0.002 (lower curve) cm. Absorption loss in the liquid is 14%; overall transmittances in the absence of a laser (i.e., t = 0) are 85 and 74%, respectively.

be a reflected wave and a transmitted wave. For the coordinates shown in Fig. 6, the interface is the x-y plane, the interface normal is the z axis, and the wave vectors of the waves lie in the x-z plane.

The reflected angle Θ_r and the transmitted angle Θ_t are related to the incident angle Θ_i as

$$\Theta_r = \Theta_i \tag{34}$$

$$\Theta_t = \sin^{-1} \left(\frac{\sin\Theta_i}{n}\right) \tag{35}$$

where

$$n = \frac{n_b}{n_a} \tag{36}$$

n_a and n_b are the indices of refraction of the two media, and n is the relative index of refraction.

In general, EM waves can be resolved into two components with polarizations perpendicular to each other. Reflectance and transmissivity at the interface depend on the polarization. For transverse electric (TE) polarization, in which the electric vector of the incident wave is parallel to the interface, the transmissivity and the reflectance are given by

$$T_{TE} = 1 - R_{TE} \tag{37}$$

$$R_{TE} = \left| \frac{\cos\,\Theta_i - \sqrt{n^2 - \sin^2\Theta_i}}{\cos\,\Theta_i + \sqrt{n^2 - \sin^2{}_i\theta}} \right|^2 . \tag{38}$$

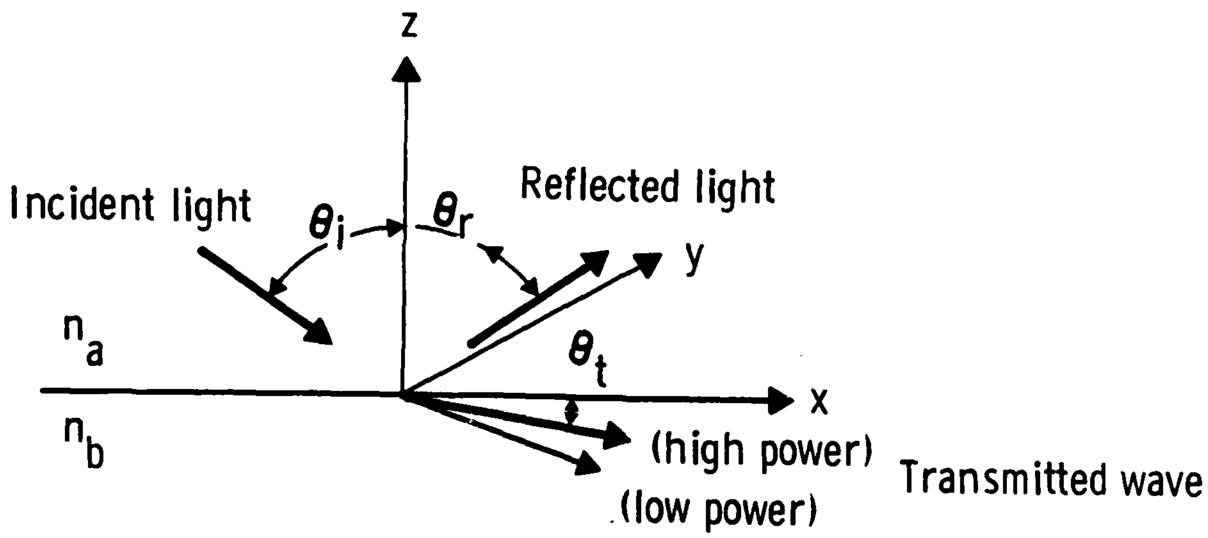

Figure 6. Schematic diagram of the nonlinear interface. Media a and b occupy the regions Z > 0 abd < 0, respectively.

For transverse magnetic (TM) polarization, in which the magnetic vector of the incident wave is parallel to the interface, the transmissivity and the reflectance are given by

$$T_{TM} = 1 - R_{TM} \tag{39}$$

$$R_{TM} = \left| \frac{n^2 \cos\theta_i - \sqrt{n^2 - \sin^2\theta_i}}{n^2 \cos\theta_i + \sqrt{n^2 - \sin^2\theta_i}} \right|^2 . \tag{40}$$

Transmissivity and reflectance of an EM wave without specific polarization are given by their average value

$$T = 1/2\,(T_{TE} + T_{TM}) \tag{41}$$

$$R = 1/2\,(R_{TE} + R_{TM}). \tag{42}$$

Equations (38) and (40) clearly show that transmissivity and reflectance depend on n and θ_i for both the TE and TM cases. Although the actual functions are different, transmission and reflection for both polarizations have a common feature: total internal reflection occurs for both cases when $n < 1$ and $\theta_i > \theta_c$, where

$$\theta_c = \sin^{-1}(n). \tag{43}$$

Only cases in which medium b is nonlinear and has a negative n_2, i.e., $n_b = n_{bo} + n_2 I$, will be discussed here. However, since Eqs. (38) and (40) depend only on n, the results can be easily extended to cases with positive n_2 as well as to cases where "a" is the nonlinear medium and "b" is the linear medium.

Substituting n_b into Eq. (43) gives the power density-dependent θ_c as

$$\theta_c(I) = \sin^{-1} \frac{n_{bo} + n_2 I}{n_a} . \tag{44}$$

In other words, when the incident power density increases, the critical angle θ_c decreases. If the incident angle θ_i is selected to be less than $\theta_c(0) = \sin^{-1} (n_{bo}/n_a)$, a low-power beam will be transmitted through the interface; but as power density increases and the critical angle decreases and becomes closer to θ_i, transmissivity is reduced. Further increases in I shift θ_c to angles less than θ_i and result in total internal reflection, i.e., the optical density of the limiter becomes infinite since no transmission is possible.

Figure 7 shows the theoretical transmission through a nonlinear interface for various incident angles. At large θ_i, transmissivity changes are more abrupt when I increases. For example, when $\theta_i = 80^0$ and $n_{bo}/n_a = 0.988$, the low power transmissivity is higher than 80%. But, a change in n of as little as 0.002 due to an intensity increase completely blocks the high-power incident beam. At $\theta_i = 60^0$ and $n_{bo}/n_a = 0.885$, transmissivity can also be higher than 80%. However, n must change by at least 0.021 to produce total internal reflection of the interface. Therefore, the larger θ_i is preferred for optical switching because the threshold power density needed to cause switching from high transmissivity to total internal reflection is smaller. However, a selection of large θ_i will limit us to a small field of view. The changes in indices of refraction needed at various θ_i to switch the interface from 80% transmission to total reflection for a TE wave are listed in Table 1. The changes required for a TM wave are somewhat smaller.

Some degree of switching can also be achieved by an increase in θ_t, which is induced by an increase in the intensity dependent n_a. Substituting n_b into Eq. (35), we obtain

$$\theta_t = \sin^{-1} \left(\frac{n_a \sin\theta_i}{(n_{bo} + n_2 I)} \right) . \tag{45}$$

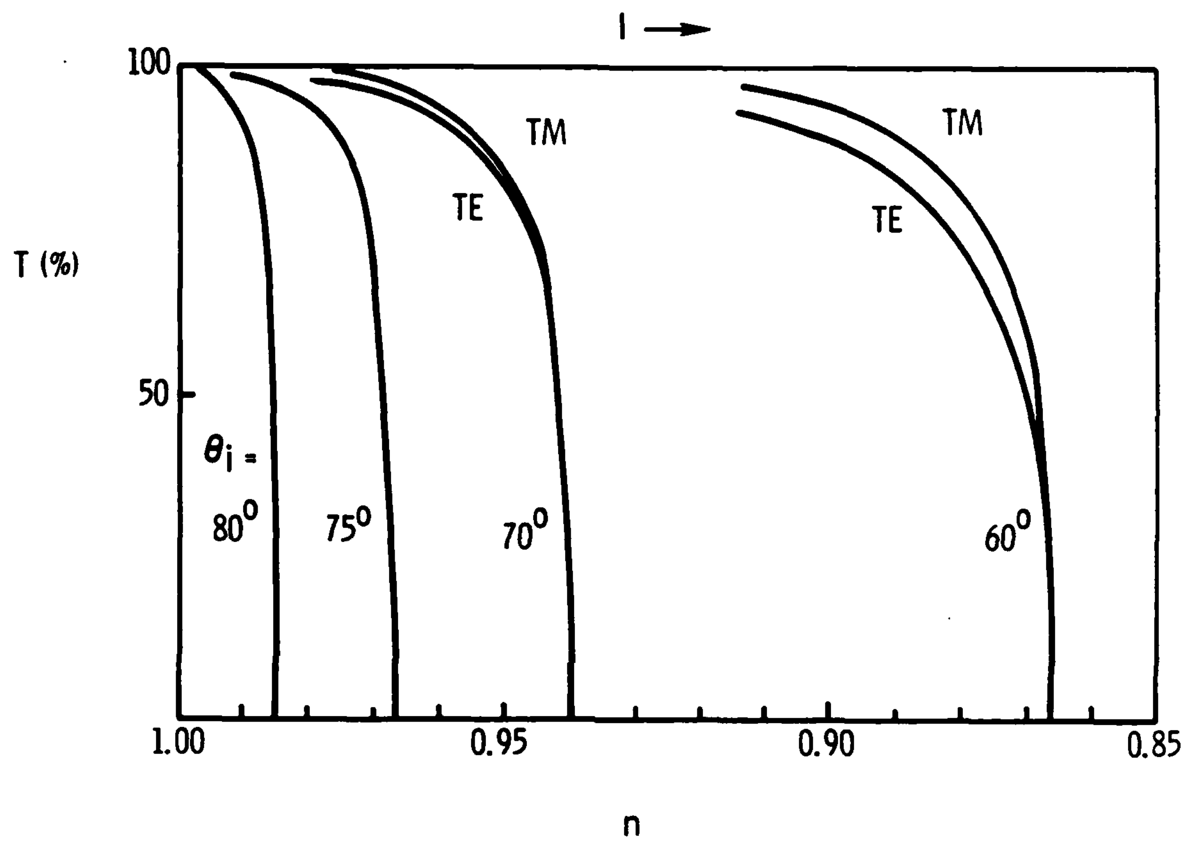

Figure 7. Transmission vs relative refractive index, n, for various incident angles θ_i. Note that n decreases as I increases.

Table 1

Change in Indices of Refraction, Δn, Needed for Switching an Interface from 80% Transmission to Total Internal Reflection for a TE Wave

Θ_i (degrees)	$n_{80\%}$ [a]	n_c [b]	Δn [c]
89	0.99987	0.99985	-0.0002
88	0.99948	0.99939	-0.0009
87	0.99883	0.99863	-0.00020
86	0.99792	0.99756	-0.00036
85	0.99675	0.99619	-0.00056
80	0.98704	0.98481	-0.00213
75	0.97097	0.96593	-0.00904
70	0.94873	0.93969	-0.00904
65	0.92057	0.90631	-0.01426
60	0.88683	0.86603	-0.0208

a) Relative index at which T = 80%
b) Relative index at which total internal reflection occurs
c) $\Delta n = n_c - n_{80\%}$

As shown in Table 2 for $\Theta_i = 60°$, the resultant Θ_t is 77.56° for a low-power beam. A change in n of only 0.0135 will deflect the transmitted beam 5°, so that Θ_t becomes 82.56°. With $\Theta_i = 70°$ and $\Theta_t = 82.09°$ for a low-power beam, the required change in n can be even smaller (0.00782) to deflect the beam the same 5°. As shown in Fig. 3, such a change in n can occur in 100 μsec or less for a 0.38-W laser focused to 40 μm in diameter. Therefore, the nonlinear-interface phenomenon is also fast.

Table 2

Change in Indices of Refraction, Δ_n, Needed for the Transmitted Beam to Bend 5°

	Low Power		High Power	
R_i (degrees)	$n_{80\%}$	Θ_t	$\Theta_t = \Theta_t + 5°$	(Δ_n)
75	0.97087	84.16	89.16	-0.0049
70	0.94873	82.09	87.06	-0.0078
65	0.92057	79.90	84.90	-0.0107
60	0.88683	77.56	82.56	-0.0135

IV. CONCLUSION

We have analyzed two dynamic nonlinear optical effects, artificial Kerr and photothermal, and reviewed two nonlinear phenomena, self-defocusing and nonlinear interface. The generic results are summarized below. Please see Volume II for their device applications.

- As far as we know, we are the first to derive the dynamic nonlinear coefficient n_2' of AKM.
- We found that the figure of merit of AKM should be defined as $n_2/\alpha_0\lambda_0$ and not the n_2/α_0 originally used in Ref. 6 because α_0 cannot be infinitely increased.
- The dynamic nonlinear coefficient n_2' is larger for smaller spheres under the constraint of the same scattering loss.
- Although both AKM and absorptive liquid mixtures are highly nonlinear optical materials, the photothermal effect of the latter is about three orders of magnitude higher under the same focus condition.
- Both the self-defocusing and nonlinear-interface phenomena produce a response faster than 100 μsec under reasonable power levels.

V. REFERENCES

1. See Optical Eng., 24, (4), 1985.

2. A. Ashkin, J.M. Dziedzic, and P.W. Smith, Opt. Lett. 7, 276 (1982).

3. J.A. Stratton, Electromagnetic Theory (McGraw-Hill, New York, 1941).

4. J.P. Gordon, Phys. Rev. A8, 14 (1973).

5. M. Kerker, The Scattering of Light (Academic Press, New York, 1969), p. 37.

6. P.W. Smith, P.J. Maloney, and A. Ashkin, Opt. Lett. 7, 347 (1982).

7. A.E. Siegman, An Introduction to Lasers and Masers (McGraw Hill, New York, 1971), p. 309.

8. H.L. Fang and R.L. Swofford, Ultrasensitive Laser Spectroscopy, Chap. 3 (Academic Press, NY), 175 (1983).

9. K. Raznievic, Handbook of Thermodynamic Tables and Charts (Hemisphere Publishing Co., Washington) (1976).

10. D. Beysens and P. Calmettes, J. Chem. Phys. 66, 766 (1977).

11. R.K. Jain and D.G. Steel, Appl. Phys. Lett. 37, 1 (1980).

12. J.P. Gordon, R.C.C. Leite, R.S. Moore, S.P.S. Porto, and J.R. Whinnery, J. Appl. Phys. 36, 3 (1965).

13. J.R. Whinnery, Accts. Chem. Res. 7, 225 (1974).

14. J.M. Harris and N.J. Dovichi, Anal. Chem. 52, 695A (1980).

15. A.E. Kaplan, JETP Lett. 24, 114 (1976).

END
8-87
DTIC